DYNAMIC ANALYSIS AND PEAK PREDICTION OF THE 6-DOF BIONIC MANIPULATOR

Bingyan CUI[1,2,3]*, Liwen CHEN[1, 2], Yongtao XIE[2], Zhijun WANG[2],

In order to solve the problem of the complex structure and weak bearing capacity of bionic manipulator, a novel 6-DOF bionic manipulator is proposed, which with 3-UPS kinematic chains connecting the moving platform to the base can reduce interference while still maintaining 6-DOF. First, the virtual prototype and the structure diagram of the manipulator are description and the kinematics equation is deduced. Secondly, the dynamic equation of a 6-DOF bionic manipulator based on the Lagrange equation is produced, the peak prediction model is derived, and the dynamic character of the 6-DOF bionic manipulator is alyzed . The resulsts of actuator force/torqueof numerical simulation show that, for a given motion cuive, the peak prediction model was validated, and obtained that maximum estimated peak force and torque. Analysis results provide necessary information for dynamic performance analysis of the 6-DOF bionic manipulator. The peak prediction model can provide theoretical base for the servo motor selection.

Keywords: Bionic manipulator; 3-UPS; Lagrange; Dynamics simulation; Peak forecast.

1. Introduction

The bionic manipulator can realize grasping operation, used in mechanical processing, aerospace, metallurgy and automobile, such as [1,2]. Dynamic analysis is mainly to study the dynamic characteristics of the bionic manipulator. The mathematical model of mechanism dynamics can be established according to various mechanical principles, and the dynamic analysis method of bionic manipulator have Lagrange, Newton Euler, and Kaneand so on [3-6]. Staicu Stefan *et al*[7-9]. proposed a new dynamic modeling method based on the iterative matrix method, and analyzed dynamics equation of the spherical 3-UPS/S parallelmechanism and a mobile robot.

The dynamic equations established by Newton Euler method are convenient to calculate the inverse solution of parallel mechanism [10]. Sugimoto [11] established the rigid body dynamics model of Stewart mechanism by using the

[1] Yanshan University, Qinhuangdao 064000, China.
[2] North China University of Science and Technology, Tangshan 063009,China.
[3] Widex Sanitary Co., Ltd., Tangshan 063000,China.
E-mail: mj_cby@sina.com, liwenchen2003@126.com, 851574051@qq.com,zjwang@ncst.edu.cn

Newton-Euler method. Zhang *et al*.[12] have derived for dynamic model of 6-PSS parallel earthquake simulator based on the Newton - Euler method. Feng, *et al.* [13] established dynamic equation of 3PUS-S(P) the spherical metamorphic mechanism, the driving forces and constrained forces were obtained [14,15].

It is relatively easy to solve the dynamic inverse solution of bionic manipulator using rigid body dynamics's the principle of virtual work method. Tsai derived the equation of solving the inverse dynamics, and the dynamic model is reduced a six linear equations [16]. GALLARDO [17] proposed an analysis method of parallel robot dynamics use of the principle of virtual work. XK Song, *et al* [18] dervied the dynamical model of the 4PUS- 1RPU manipulator, and drawn the simulation diagram of the inverse dyanimc characetristics.

Lagrange method with generalized coordinates can describe the overall system movement equation. LEE *et al*.[19] had analyzed of the 3-RPS mechanism for the kinematics and dynamics by Lagrange method. By Lagrange method and first order, two order motion influence coefficient. Thanh *et al* [20] introduced a dynamic modeling method of parallel mechanism based on Lagrange equations. Cui *et al* [21, 22] presented a hip joint and deduced the dynamics model of hip joint mechanism and obtained its dynamical characteristics.

The 6-DOF bionic manipulator adopts a 3-UPS parallel mechanism as a prototype, which is a deformation of the Stewart mechanism and reduces the structure of the three UPS branches compared to their simple structure and has the characteristics of 6-DOF motion. Three DC servo motors fixed on the Hooke hinge are installed on the rack to reduce inertia. According to the analysis of reference [23,24], the parallel mechanism has better bearing capacity than the traditional series mechanical manipulator, and has good carrying capacity.

This paper proposes a 6-DOF bionic manipulator, has the advantage of the flexibility of motion, and makes the bionic manipulator more easy control. The carrying capacity of bionic manipulator with parallel structure is much larger than traditional serial manipulator. This paper establishes the kinematic equation and dynamic equation, and the driving speed and driving force of servo motor are predicted based on the dynamic characteristics, the peak value of its driving parameters is obtained.

2 Structure descriptions of bionic manipulator and kinematic solution

2.1 Structure description of bionic manipulator

A 6-DOF bionic manipulator virtual prototype is shown in Fig.1. The working principle of the 6-DOF manipulator is driven by three prismatic hinges and three rotating hinge.

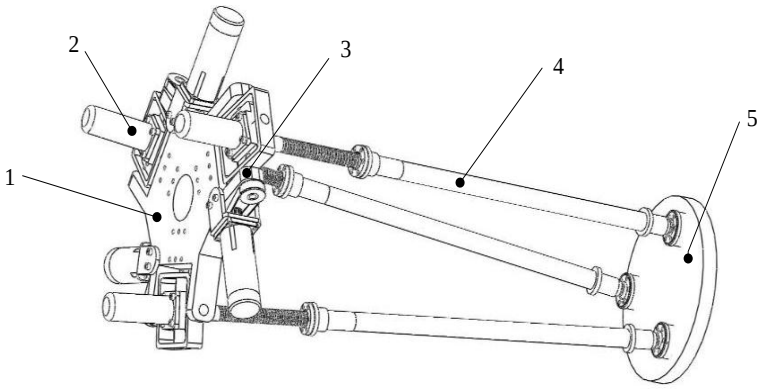

1 – static platform 2– servo motors 3– belt drive mechanism 4– UPS kinematic chain 5– moving platform
Fig. 1 The 6-DOF bionic manipulator mechanism

This 6-DOF bionic manipulator consists of static platform, 3-UPS branches and moving platform, as shown in Fig. 2. Each branch chain comprises Hooke hinge U_i, prismatic hinge P_i, and ball hinge S_i, which are respectively connected with a static platform, upper - lower connecting rod and a moving platform. The distribution of Hooke hinge point on the static platform is equilateral triangle, and the fixed platform $U_1U_2U_3$ of the circum radius is a. The distribution of ball hinge point on the moving platform is equilateral triangle too, and the outer radius of moving platform $S_1S_2S_3$ is b.

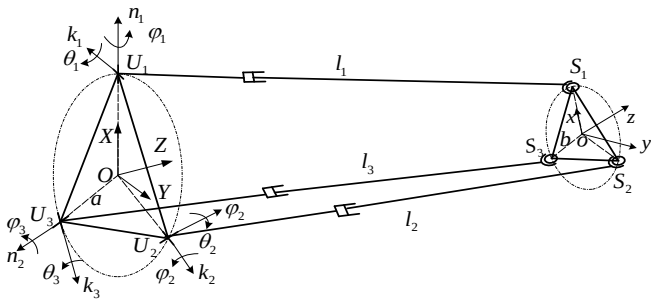

Fig. 2 The structure of 6-DOF bionic manipulator

The coordinate is described in reference [24,25].The fixed coordinate ***K*** [*X, Y, Z*] is laid on the fixed platform $U_1U_2U_3$, the coordinate origin O is located at the center of the fixed platform $U_1U_2U_3$, the Z axis is perpendicular to the fixed platform, the *X*-axis points to the center point U_1 of the Hooke joint, and the *Y*-axis is determined by the right hand rule. While moving coordinate system ***B***[*x, y, and z*] is established on the moving platform $S_1S_2S_3$, the coordinate origin o is rotation center of the moving platform, the *z* axis is perpendicular to the moving platform, the *x*-axis points to the center point S_1 of the ball joint, and the *y*-axis is determined

by the right hand rule. The Hooke hinge U_i can described by two angle in fixed coordinate, which a rotation angle θ_i about the k_iU_i axis, followed by another rotation of angle φ_i about the rotated OU_i axis. The bionic manipulator realizes 6-DOF movement of space through the drive of three rotation joint U_ik_i axes and the drive of three prismatic hinge l_i. The three local coordinate system $\boldsymbol{B_i}$ [n_i, k_i, p_i], p_i is along the direction of the prismatic hinge, n_i is along the direction of U_in_i, k_i is along the direction of the U_in_i.

2.2 Kinematic analysis

In the fixed coordinate system $\boldsymbol{K}$, the vector equation is can be written as

$$\boldsymbol{OS}_i = \boldsymbol{OU}_i + \boldsymbol{U}_i\boldsymbol{S}_i \rightarrow \boldsymbol{P} + \boldsymbol{b_i} = \boldsymbol{u_i} + \boldsymbol{l_i} \quad (i=1, 2, 3). \tag{1}$$

Where, $\boldsymbol{OS}_i = \boldsymbol{Oo} + \boldsymbol{RoS}_i$, $\boldsymbol{R}$ is homogeneous transformation matrix. $\boldsymbol{P}$ is the position vector of the moving platform in the fixed coordinate system, $\boldsymbol{u_i}$ is the position vector of the Hooke joint center U_i in the fixed coordinate system, $\boldsymbol{u}_i = \begin{pmatrix} a\cos\eta_i & a\sin\eta_i & 0 \end{pmatrix}$. $\boldsymbol{b_i}$ is the position vector of the ball hinge center S_i, $\boldsymbol{l}_i$ is vector of the branch in fixed coordinate system.

The derivative of the formula (1), the formula is deduced as

$$\boldsymbol{v} + \boldsymbol{\omega} \times \boldsymbol{b}_i = \dot{\boldsymbol{l}}_i \boldsymbol{p}_i \quad (i=1, 2, 3). \tag{2}$$

Where, $\dot{\boldsymbol{l}}_i$ is input speed of mobile drive motion, $\boldsymbol{p}_i$ is the unit vector of the extension direction, $\boldsymbol{\omega}$ is the angular velocity of the output of the moving platform.

According the formula (1), the vector formula can be written as

$$\dot{\boldsymbol{l}}_i = \boldsymbol{v} \cdot \boldsymbol{p}_i + \boldsymbol{\omega}\left(\boldsymbol{b}_i \times \boldsymbol{p}_i\right) = \boldsymbol{D}_1 \begin{bmatrix} \boldsymbol{v}^{\mathrm{T}} & \boldsymbol{\omega}^{\mathrm{T}} \end{bmatrix}^{\mathrm{T}} \quad (i=1, 2, 3). \tag{3}$$

Where, $\dot{\boldsymbol{l}}_i = \begin{bmatrix} \dot{l}_1 & \dot{l}_2 & \dot{l}_3 \end{bmatrix}^{\mathrm{T}}$, $\boldsymbol{D}_1 = \begin{bmatrix} \boldsymbol{p}_1^{\mathrm{T}} & \left(\boldsymbol{b}_1 \times \boldsymbol{p}_1\right)^{\mathrm{T}} \\ \boldsymbol{p}_2^{\mathrm{T}} & \left(\boldsymbol{b}_2 \times \boldsymbol{p}_2\right)^{\mathrm{T}} \\ \boldsymbol{p}_3^{\mathrm{T}} & \left(\boldsymbol{b}_3 \times \boldsymbol{p}_3\right)^{\mathrm{T}} \end{bmatrix}$, $\boldsymbol{D}_1 \in \boldsymbol{R}^{3\times 6}$.

If the output angular velocity and angular velocity of the moving platform are known, the velocity of the ball hinge point S_i can be expressed as

$$\boldsymbol{v}_{Si} = \boldsymbol{\omega} \times \boldsymbol{s}_i = \boldsymbol{\omega}_{pi} \times \boldsymbol{l}_i + \dot{l}_i \boldsymbol{p}_i \quad (i=1, 2, 3). \tag{4}$$

Where, $\boldsymbol{\omega}_{pi}$ is the angle velocity of the branch, $\boldsymbol{s}_i$ is the position vector of the ball hinge center S_i in the fixed coordinate system.

According to the formula (2) and formula (4), the angular velocity of the branch is obtained by

$$\boldsymbol{\omega}_{pi} = \frac{\boldsymbol{p}_i \times (\boldsymbol{\omega} \times \boldsymbol{s}_i)}{l_i} \quad (i=1, 2, 3). \tag{5}$$

The derivative of the formula (4), the accelerate velocity of the ball hinge center S_i is deduced as

$$\boldsymbol{a}_{Si} = \dot{\boldsymbol{\omega}} \times \boldsymbol{s}_i + \dot{\boldsymbol{\omega}} \times (\dot{\boldsymbol{\omega}} \times \boldsymbol{s}_i) = \dot{\omega}_{pi} \times \boldsymbol{l}_i + \omega_{pi} \times (\omega_{pi} \times \boldsymbol{l}_i) + \ddot{l}_i \boldsymbol{p}_i \quad (i=1, 2, 3). \tag{6}$$

Where, $\dot{\omega}_{pi}$ is the angle accelerate velocity of the branch, $\ddot{l}_i$ is the linear accelerate velocity of the branch.

Formula (6) point multiply and cross-product $\boldsymbol{p}_i$, respectively, the linear velocity and accelerate velocity of the branch can be written as

$$\ddot{l}_i = \boldsymbol{a}_{Si} \cdot \boldsymbol{p}_i + l_i \boldsymbol{\omega}_{pi} \cdot \boldsymbol{\omega}_{pi} \quad (i=1, 2, 3). \tag{7}$$

$$\dot{\boldsymbol{\omega}}_{pi} = \frac{\boldsymbol{p}_i \times \boldsymbol{a}_{Si} - 2\dot{\boldsymbol{l}}_i \cdot \boldsymbol{\omega}_{pi}}{l_i} \quad (i=1, 2, 3). \tag{8}$$

Based on the angular velocity superposition principle, the angular velocity of the branch is calculated as

$$\boldsymbol{\omega}_{pi} = \dot{\varphi}_i \boldsymbol{n}_i + \dot{\theta}_i \boldsymbol{k}_i \quad (i=1, 2, 3). \tag{9}$$

Where, $\boldsymbol{n}_i$ is the unit vector of the n_i axis in fixed coordinate system, $\boldsymbol{k}_i$ is the unit vector of the k_i axis in fixed coordinate system.

Formula (9) cross-product $\boldsymbol{n}_i$, use of the formula (5), can be deduced as

$$\dot{\boldsymbol{\theta}}_i = \frac{\boldsymbol{s}_i}{l_i (\boldsymbol{k}_i \times \boldsymbol{n}_i)} \boldsymbol{\omega} = \boldsymbol{D}_2 \begin{bmatrix} \boldsymbol{v}^{\mathrm{T}} & \boldsymbol{\omega}^{\mathrm{T}} \end{bmatrix}^{\mathrm{T}} \quad (i=1, 2, 3). \tag{10}$$

Where, $\dot{\boldsymbol{\theta}}_i = \begin{bmatrix} \dot{\theta}_1 & \dot{\theta}_2 & \dot{\theta}_3 \end{bmatrix}^{\mathrm{T}}$, $\boldsymbol{D}_2 = \begin{bmatrix} 0 & \dfrac{\boldsymbol{s}_1^{\mathrm{T}}}{l_1(\boldsymbol{k}_1 \times \boldsymbol{n}_{i1})} \\ 0 & \dfrac{\boldsymbol{s}_2^{\mathrm{T}}}{l_2(\boldsymbol{k}_2 \times \boldsymbol{n}_2)} \\ 0 & \dfrac{\boldsymbol{s}_3^{\mathrm{T}}}{l_3(\boldsymbol{k}_3 \times \boldsymbol{n}_3)}^{\mathrm{T}} \end{bmatrix}$, $\boldsymbol{D}_2 \in \boldsymbol{R}^{3\times 6}$.

From formula (5) and formula (6), the speed mapping relationship of the bionic manipulator can be obtained as

$$\dot{\boldsymbol{\zeta}} = \boldsymbol{D}\boldsymbol{V} . \tag{11}$$

Where, $\boldsymbol{D}$ is Jacobian matrix, $\boldsymbol{D} = \begin{bmatrix} \boldsymbol{D}_1 & \boldsymbol{D}_2 \end{bmatrix}^{\mathrm{T}}$ and $\boldsymbol{D} \in \boldsymbol{R}^{6\times 6}$, $\dot{\boldsymbol{\zeta}}$ is input velocity vector of bionic manipulator, $\dot{\boldsymbol{\zeta}} = \begin{bmatrix} \dot{\boldsymbol{l}} & \dot{\boldsymbol{\theta}} \end{bmatrix}^{\mathrm{T}}$, $\boldsymbol{V}$ is generalized output speed vector of the moving platform, $\boldsymbol{V} = \begin{bmatrix} \boldsymbol{v} & \boldsymbol{\omega} \end{bmatrix}^{\mathrm{T}}$.

The influence of manipulator's kinematic equation and structural parameters is described in detail in reference [24].

3 Dynamic analysis of 6-DOF bionic manipulator mechanism

According to the literature [26] in this paper, the Lagrange method is used to analyze the dynamics of bionic manipulator. Assuming the connecting rods are uniform density and regular shape, and ignoring the influence of friction.

3.1 The potential energy of 6-DOF bionic manipulator

3.1.1 The potential energy of the moving platform

The moving platform is a regular cylinder structure with the center of mass as the center of the geometric shape. In fixed coordinate system, m_c is quality of the moving platform.

The potential energy of the moving platform is defined as

$$Q_d = m_c g \boldsymbol{r}_{c0} . \tag{12}$$

Where, $\boldsymbol{r}_{c0}$ is the centroid position vector of the moving platform.

3.1.2 The potential energy of the 3-UPS branched chain

The potential energy of the bionic manipulator UPS branched chain is composed of Hookehinge component, lead screw and forearm rod. The Hookehinge

component, lead screw and forearm rod can rotate around the center of Hookehinge point U_i, and the telescopic rod is connected to the lead screw through the prismatic hinge, and can move along the lead screw. The potential energy of the UPS branched chain is defined as

$$Q_{Fi} = (m_u g \boldsymbol{r}_{uiz} + m_s g \boldsymbol{r}_{siz} + m_t g \boldsymbol{r}_{tiz}) \quad (i = 1, 2, 3). \tag{13}$$

Where, the quality of Hooke hinge component is m_u, the overall quality of lead screw and motor rotor is m_s, the telescopic rod quality is m_t, the centroid positive vector of the Hooke hinge is $\boldsymbol{r}_{uiz}$, the centroid position vector of lead screw and motor rotor is $\boldsymbol{r}_{siz}$, the centroid position vector of the telescopic rod is $\boldsymbol{r}_{tiz}$.

3.1.3 The total potential energy of the 6-DOFbionic manipulator

The total potential energy of the 6-DOFbionic manipulator can be expressed as

$$Q_t = \sum_{i=1}^{3} Q_{Fi} + Q_d \quad . \tag{14}$$

3.2 The kinetic energy of the bionic manipulator

3.2.1 The kinetic energy of the moving platform

The moving platform of the 6-DOF bionic manipulator can realize the three-dimensional movement and the three-dimensional rotation, so the moving platform contains two aspects of kinetic energy of linear velocity and angular velocity. The kinetic energy of the 6-DOF manipulator moving platform is defined as

$$E_d = \frac{1}{2} m_c \boldsymbol{v}^2 + \frac{1}{2} \boldsymbol{\omega}^{\mathrm{T}} \boldsymbol{J}_c \boldsymbol{\omega} . \tag{15}$$

Where, output centroid angular velocity of the moving platform is $\boldsymbol{\omega}$, the output centroid linear velocity of the moving platform is $\boldsymbol{v}$, $\boldsymbol{J}_c$ is the inertial tensor of the moving platform.

3.2.2 The kinetic energy of the UPS branched chain

The Hooke hinge component rotate around the center Hookehinge, the kinetic energy of the Hookehinge component in fixed coordinate system is defined as

$$E_{Ui} = \frac{1}{2} \boldsymbol{\omega}_{pi}^{\mathrm{T}} \left(\boldsymbol{J}_{Ui} \right) \boldsymbol{\omega}_{pi} \quad (i = 1, 2, 3). \tag{16}$$

Where, $\boldsymbol{J}_{Ui}$ is the inertial tensor of the Hooke hinge component around rotating the center of Hooke hinge point U_i.

The lead screw and motro rotor can realize the rotational movement around the center of Hookehinge. So the lead screw contains two aspects of kinetic energy of angular velocity of Hookehinge and its rotating angular velocity. The kinetic energy of the 6-DOF manipulator lead screw is defined as

$$E_{Si} = \frac{1}{2}\boldsymbol{\omega}_{pi}^{\mathrm{T}}\left(\boldsymbol{J}_{si}\right)\boldsymbol{\omega}_{pi} + \frac{1}{2}\boldsymbol{\omega}_{sci}{}^{\mathrm{T}}\boldsymbol{J}_{sci}\boldsymbol{\omega}_{sci} \quad (i=1,2,3). \tag{17}$$

Where, the rotation angular velocity of the lead screw and motor rotor is $\boldsymbol{\omega}_{sci}$, which rotate around its own axis. $\boldsymbol{J}_{si}$ is inertial tensor of the lead screw and motor rotor around rotating the center of Hooke hinge point U_i, $\boldsymbol{J}_{sci}$ is the inertial tensor of the lead screw and motor rotor around rotating its own axis.

The telescopic rod contains two aspects of kinetic energy of angular velocity of Hookehinge and its rotating angular velocity. The kinetic energy of the telescopic rod is defined as

$$E_{fi} = \frac{1}{2}\boldsymbol{\omega}_{pi}^{\mathrm{T}}\left(\boldsymbol{J}_{fi}\right)\boldsymbol{\omega}_{pi} + \frac{1}{2}m_t\boldsymbol{v}_{ti}^2 \quad (i=1,2,3). \tag{18}$$

Where, the inertial tensor of telescopic rod around its centroid vertical axis is $\boldsymbol{J}_{fi}$, the centroid velocity of the telescopic rod is $\boldsymbol{v}_{ti}$.

3.2.3 The total kinetic energy of the 6-dof bionic manipulator

The total kinetic energy of the 6-DOF bionic manipulator can be expressed as

$$E_t = E_d + \sum_{i=1}^{3} E_{Ui} + \sum_{i=1}^{3} E_{Si} + \sum_{i=1}^{3} E_{fi}. \tag{19}$$

3.3 Lagrange equation and dynamic model of the 6-DOF bionic manipulator

According to the Lagrange function, L is defined as the difference between of the system the total kinetic energy E_t and the total potential energy Q_t. L is written as

$$L = E_t - Q_t. \tag{20}$$

In referenc [8], the dynamics of the 3-UPS/S mechanism are analyzed using the Lagrangian method. The establishment of a coordinate system is different. Therefore, there are differences in the calculation formulae of kinetic energy and potential energy in the 3 -UPS. The formular(28) in reference[8] corresponds to the

difference between their corresponding kinetic energy and potential energy. The kinetic energy and potential energy in the reference formula (28) correspond to the formula(12)、formula(13) and formulas(15) to formulas(18) in the paper, but the form of expression is different becouse of the difference of coordinate system.

By using of the second Lagrange equation[19], the system dynamics equation of 6-DOF bionic manipulator is established as

$$\boldsymbol{F}_g = \frac{\partial}{\partial t}\left(\frac{\partial L}{\partial \dot{\boldsymbol{q}}}\right) - \frac{\partial L}{\partial \boldsymbol{q}} \ . \tag{21}$$

Where, $\boldsymbol{F}_g$ is generalized output force.

Based on system dynamics equation (21), the kinetic energy, the potential and the corresponding generalized force of each component of the 6-DOF bionic manipulator are calculated.

$$\begin{aligned}\boldsymbol{F}_g &= \frac{d}{dt}\left(\frac{\partial E_t}{\partial \dot{\boldsymbol{q}}}\right) + \frac{\partial Q_t}{\partial \boldsymbol{q}} - \frac{\partial}{\partial t}\left(\frac{\partial Q_t}{\partial \dot{\boldsymbol{q}}}\right) - \frac{\partial E_t}{\partial \boldsymbol{q}} \\ &= \left[\frac{\partial}{\partial t}\left(\frac{\partial E_t}{\partial \dot{\boldsymbol{q}}}\right) - -\frac{\partial}{\partial t}\left(\frac{\partial Q_t}{\partial \dot{\boldsymbol{q}}}\right)\right] + \left[\frac{\partial Q_t}{\partial \boldsymbol{q}} - \frac{\partial E_t}{\partial \boldsymbol{q}}\right]. \\ &= \boldsymbol{H}_t\ddot{\boldsymbol{q}} + \boldsymbol{C}_{t1}\dot{\boldsymbol{q}} + \boldsymbol{C}_{t2}\dot{\boldsymbol{q}} + \boldsymbol{K}_t \\ &= \boldsymbol{H}_t\ddot{\boldsymbol{q}} + \boldsymbol{C}_t\dot{\boldsymbol{q}} + \boldsymbol{K}_t\end{aligned} \tag{22}$$

Where, $\ddot{\boldsymbol{q}}$ is generalized accelerate velocity,

$$\ddot{\boldsymbol{q}} = (\ddot{X} \quad \ddot{Y} \quad \ddot{Z} \quad \ddot{\alpha} \quad \ddot{\beta} \quad \ddot{\gamma})^{\mathrm{T}} = \left(a_x \quad a_y \quad a_z \quad \theta_\alpha \quad \theta_\beta \quad \theta_\gamma\right)^{\mathrm{T}};$$

the inertial moment of the bionic manipulator is $\boldsymbol{H}_t$,

$$\boldsymbol{H}_t = \frac{1}{2}\sum_{i=1}^{3}\left(\frac{\partial}{\partial t}\frac{\partial(\boldsymbol{\omega}_{sci}{}^{\mathrm{T}}\boldsymbol{\omega}_{sci})}{\partial \dot{\boldsymbol{q}}}\right) + \frac{3}{2}\sum_{i=1}^{3}\left(\frac{\partial}{\partial t}\frac{\partial(\boldsymbol{\omega}_{pi}{}^{\mathrm{T}}\boldsymbol{\omega}_{pi})}{\partial \dot{\boldsymbol{q}}} + \right) + \frac{1}{2}\left(m_{tc}\frac{\partial}{\partial t}\frac{\partial(\boldsymbol{v}^{\mathrm{T}}\boldsymbol{v})}{\partial \dot{\boldsymbol{q}}} + \frac{\partial}{\partial t}\frac{\partial(\boldsymbol{\omega}^{\mathrm{T}}\boldsymbol{\omega})}{\partial \dot{\boldsymbol{q}}}\right),$$

The centrifugal and Coriolis forces of the bionic manipulator is $\boldsymbol{C}_t, \boldsymbol{C}_t = \boldsymbol{C}_{t1} + \boldsymbol{C}_{t2}$, Which,

$$\begin{aligned}\boldsymbol{C}_{t1} = {} & \frac{1}{2}\sum_{i=1}^{3}\left(\frac{\partial}{\partial t}\frac{\partial(\boldsymbol{J}_{si})}{\partial \dot{\boldsymbol{q}}} + \frac{\partial}{\partial t}\frac{\partial(\boldsymbol{J}_{sci})}{\partial \dot{\boldsymbol{q}}}\right) + \frac{1}{2}\sum_{i=1}^{3}\left(\frac{\partial}{\partial t}\frac{\partial(\boldsymbol{J}_{fi})}{\partial \dot{\boldsymbol{q}}} + m_f\frac{\partial}{\partial t}\frac{\partial(\boldsymbol{v}_{ti}{}^{\mathrm{T}}\boldsymbol{v}_{ti})}{\partial \dot{\boldsymbol{q}}}\right) \\ & + \frac{1}{2}\left(\frac{\partial}{\partial t}\frac{\partial(\boldsymbol{J}_c)}{\partial \dot{\boldsymbol{q}}}\right) + \frac{1}{2}\sum_{i=1}^{3}\left(\frac{\partial}{\partial t}\frac{\partial(\boldsymbol{J}_{Ui})}{\partial \dot{\boldsymbol{q}}}\right) - m_{tc}g\left(\frac{\partial}{\partial t}\frac{\partial(\boldsymbol{r}_{co})}{\partial \dot{\boldsymbol{q}}}\right) \\ & - m_u g\sum_{i=1}^{3}\left(\frac{\partial}{\partial t}\frac{\partial(\dot{\boldsymbol{r}}_{uiz})}{\partial \dot{\boldsymbol{q}}}\right) - m_s g\sum_{i=1}^{3}\left(\frac{\partial}{\partial t}\frac{\partial(\dot{\boldsymbol{r}}_{siz})}{\partial \dot{\boldsymbol{q}}}\right) - m_t g\sum_{i=1}^{3}\left(\frac{\partial}{\partial t}\frac{\partial(\dot{\boldsymbol{r}}_{tiz})}{\partial \dot{\boldsymbol{q}}}\right)\end{aligned} \ ,$$

$$\boldsymbol{C}_{t2}=-\frac{1}{2}\sum_{i=1}^{3}\left(\frac{\partial(\boldsymbol{J}_{fi})}{\partial\boldsymbol{q}}+\frac{\partial(\boldsymbol{\omega}_{pi}{}^{\mathrm{T}}\boldsymbol{\omega}_{pi})}{\partial\boldsymbol{q}}+m_{tg}\frac{\partial(\boldsymbol{v}_{ti}{}^{\mathrm{T}}\boldsymbol{v}_{ti})}{\partial\boldsymbol{q}}\right)+\frac{1}{2}\sum_{i=1}^{3}\left(\frac{\partial(\boldsymbol{J}_{Ui})}{\partial\boldsymbol{q}}+\frac{\partial(\boldsymbol{\omega}_{pi}{}^{\mathrm{T}}\boldsymbol{\omega}_{pi})}{\partial\boldsymbol{q}}\right)$$
$$-\frac{1}{2}\sum_{i=1}^{3}\left(\frac{\partial(\boldsymbol{J}_{si})}{\partial\boldsymbol{q}}+\frac{\partial(\boldsymbol{\omega}_{pi}{}^{\mathrm{T}}\boldsymbol{\omega}_{pi})}{\partial\boldsymbol{q}}+\frac{\partial(\boldsymbol{J}_{sci})}{\partial\boldsymbol{q}}+\frac{\partial(\boldsymbol{\omega}_{sci}{}^{\mathrm{T}}\boldsymbol{\omega}_{sci})}{\partial\boldsymbol{q}}\right)$$
$$-\frac{1}{2}\left(m_c\frac{\partial(\boldsymbol{v}^{\mathrm{T}}\boldsymbol{v})}{\partial\boldsymbol{q}}+\frac{\partial(\boldsymbol{J}_c)}{\partial\boldsymbol{q}}+\frac{\partial(\boldsymbol{\omega}^{\mathrm{T}}\boldsymbol{\omega})}{\partial\boldsymbol{q}}\right)$$

The gravity component of the bionic manipulator is $\boldsymbol{K}_t$,

$$\boldsymbol{K}_t=m_cg\left(\frac{\partial(\boldsymbol{r}_{co})}{\partial\boldsymbol{q}}\right)-m_ug\sum_{i=1}^{3}\left(\frac{\partial(\boldsymbol{r}_{uiz})}{\partial\boldsymbol{q}}\right)-m_sg\sum_{i=1}^{3}\left(\frac{\partial(\boldsymbol{r}_{siz})}{\partial\boldsymbol{q}}\right)-m_tg\sum_{i=1}^{3}\left(\frac{\partial(\boldsymbol{r}_{tiz})}{\partial\boldsymbol{q}}\right). \quad (23)$$

Statics equation of the 6-DOF bionic manipulator is established as

$$\boldsymbol{F}_g=\boldsymbol{G}\boldsymbol{f}_t. \quad (24)$$

Where, $\boldsymbol{f}_t$ is driver input torque, $\boldsymbol{G}$ is force Jacobian matrix, $\boldsymbol{G}=\left(\boldsymbol{D}^{-1}\right)^{\mathrm{T}}$.

Servo motor torque of the 6-DOF bionic manipulator is expressed as

$$\boldsymbol{f}_t=\boldsymbol{D}\left(\left[\boldsymbol{H}_t\right]\left[\ddot{\boldsymbol{q}}\right]+\left[\boldsymbol{C}_t\right]\left[\dot{\boldsymbol{q}}\right]+\boldsymbol{K}_t\right). \quad (25)$$

4. Peak forecast model of servo motor

In the formula(25), the effect of the centrifugal and Coriolis forces on the input torque of the motor is very small, can ignore them. So, the 6-DOF manipulator's peak torque formula can be defined as

$$\boldsymbol{f}_t=\boldsymbol{D}\left(\left[\boldsymbol{H}_t\right]\left[\ddot{\boldsymbol{q}}_t\right]+\boldsymbol{K}_t\right). \quad (26)$$

According the reference [25], the model for predicting the peak value of the servo motor is

$$\left\|\boldsymbol{f}_t\right\|_{\max}\le\left\|\boldsymbol{D}\right\|_{\max}\left\|\boldsymbol{H}_t\right\|_{\max}\left\|\ddot{\boldsymbol{q}}\right\|_{\max}+\left\|\boldsymbol{D}\right\|_{\max}\left\|\boldsymbol{K}_t\right\|_{\max}. \quad (27)$$

The 6-DOF bionic manipulator's structure parameters are a=120mm, b=50mm, $\Delta l_i=300\text{mm}$, $h=600\text{mm}$. The material of the ball screw is equal to the homogeneous bearing steel and the density is 7.81kg/m^3. Telescopic rods and motors seat are made of aluminum alloy with a density of 2.88 kg/m^3. The remaining parts of the material used 40Cr with a density of 7.8kg/m^3.

From the formulas(1) to (26) obtain the values of the variables, according to the formula (27), the maximum driving force of mobile servo motors and the

maximum driving torque of rotary servo motors for bionic manipulators can be obtained $\|\boldsymbol{f}\|_{\max}=0.297\text{N}$ and $\|\tau\|_{\max}=1.497\text{N.mm}$.

5. Simulation experiment verification

According to the function requirements of the 6-DOF bionic manipulator to achieve the function of crash, the movement trajectory is planned as

$$\begin{cases} X(t)=20\cos(\pi t/2) & (\text{rad}) \\ Y(t)=10\cos(\pi t/3) & (\text{rad}) \\ Z(t)=100\sin(\pi t/2) & (\text{rad}) \end{cases}. \tag{28}$$

Based on the formula (28), through the programming calculation of the kinetic equation (11) by MATLAB, the curve of the velocity variation of the servomotors of the three moving pairs and three rotating pairs of the bionic manipulator can be calculated as shown in Fig. 3. From Fig. 3 can be seen as velocity and angle velocity curves of the driver motor had presents periodic variation.

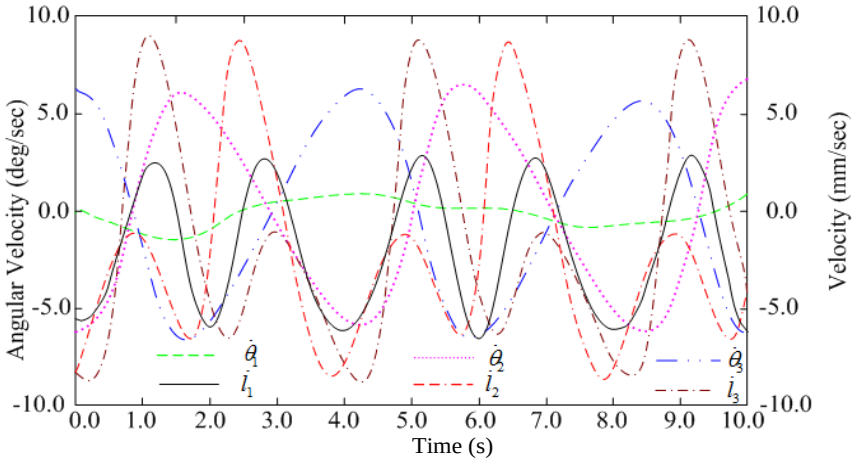

Fig.3 The velocity and angle velocity curves of the driver motor

Base on the formula(28), according the dynamic equation (26) of the 6-DOF bionic manipulator, use of Matlab the force and torque curves of the driver motor obtained, shown in Fig.4. As shown in Fig. 4, the driving force and the driving torque are periodically changed.

In order to In order to verify the correctness of theoretical derivation, the dynamic simulation analysis of bionic manipulator is carried out in this paper. Under the condition of a given motion curve formula(28), the curves of driving force and driving torque are obtained through Adams software, as shown in Fig. 4. From Fig. 4 can be seen as the curves obtained by the two methods are similar. These peaks are less than the maximum torque and maximum driving force

obtained by the corresponding theory, which verifies the rationality of the motor peak prediction model.

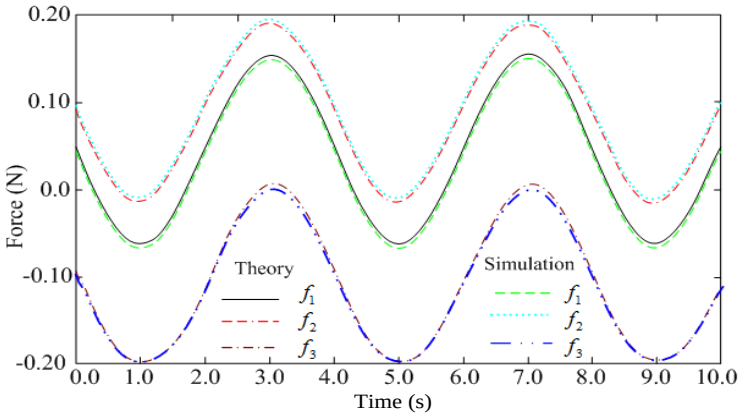

(a) The force curves of the three driver motors

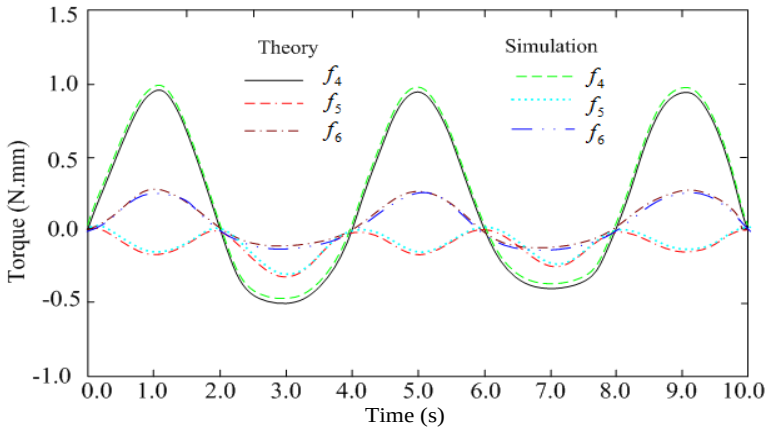

(b)The torque curves of the three driver motors

Fig.4 The force and torque curves of the driver motor

6.Conclusions

Firstly, the kinematic inverse solution of the 6-DOF bionic manipulator is deducted, and the Jacobin matrix of the bionic manipulator is deduced by the differential method. The dynamic model of bionic manipulator is established according to the Lagrangian equation and the peak model of the servo motors are proposed. The driving force and the driving torque peak of the servo motor are obtained respectively. The change rule of the bionic manipulator speed and the driving force and driving torque are analyzed when the structural parameters and the motion function are given, and the time curves of the bionic manipulator are obtained, and the maximum prediction force and torque are obtained. The

theory analysis results are compared with simulation results through an example, and the correctness and rationality of theoretical analysis are verified. This paper has good theoretical basis for further control study of the 6-DOF bionic manipulators.

Acknowledgments

This research was supported by National Natural Science Fund, (E51505124), Hebei Province Natural Science Fund (E2017209252 and E2017209059), Hebei Province Department of Education Research Fund (QN2015203and 2015GJJG084), Ministry of Education Online Education Research Center Online Education Research Fund (2016YB117).

R E F E R E N C E S

[1]. *Shen Qiong, He Yong.* Structure Design and Kinematics Analysis of a Bio-robot Manipulator. Journal of Donghua University (Natural Science Edition), 28(1):37-40.2002

[2]. *Latifah Nurahmi; Stéphane Caro;et al.* Reconfiguration analysis of a 4-RUU parallel manipulator. Mechanism and Machine Theory, 96(6):269-289. 2016

[3]. *Staicu Stefan.* Dynamics modelling of a Stewart-based hybrid parallel robot. Advanced Robotics,2015 (14):929-938. 2015

[4]. *Xuchong Zhang, Xianmin Zhang, Zhong Chen.* Dynamic analysis of a 3- R RR parallel mechanism with multiple clearance joints. Mechanism and Machine Theory, 78(78):105-115. 2014

[5]. *H.N. Rahimi; M. Nazemizadeh,* Dynamic analysis and intelligent control techniques for flexible manipulators: a review. Advanced Robotics, 28(2):63-76. 2014

[6].*Guanglei Wu, Stéphane Caro, et al.* Dynamic modeling and design optimization of a 3-DOF spherical parallel manipulator. Robotics & Autonomous Systems, 62(10):1377-1386. 2014

[7]. *Staicu Stefan, Zhang Dan.* A novel dynamic modelling approach for parallel mechanisms analysis. Robotics and Computer-Integrated Manufacturing, 24(1):167-172. 2008

[8]. *Staicu, S.*, Dynamics of the spherical 3-UPS/S parallel mechanism with prismatic actuators. Multibody System Dynamics, 22 (2): 115-132, 2009

[9]. *Staicu, S.*, Dynamics equations of a mobile robot provided with caster wheel. Nonlinear Dynamics, 58 (1-2): 237-248, 2009

[10]. *Wang Liping, Wu Jun, Wang Jinsong.* Dynamic formulation of a planar 3-DOF parallel manipulator with actuation redundancy. Robotics and Computer-Integrated Manufacturing, 26(1): 67-73. 2010

[11]. *Sugimoto K* . Kinematic and Dynamic Analysis of Parallel Manipulators by Means of Motor Algebra. Journal of mechanisms, transmissions, and automation in design, 109 (1):3-7. 1987.

[12]. *Zhang JZ, Gao F, etal.* Dynamic Analysis and Simulation of a 6-Degree of Freedom Parallel Earthquake Simulator. Journal of Shanghai Jiaotong University, 45(09):1263-1268. 2011

[13]. *Feng Zhiyou.* Inverse dynamics of a 2UPS-2RPS parallel mechanism by Newton-Euler formulation. Transactions of the Chinese Society for Agricultural Machinery, 40(4): 193-197. 2009

[14]. *Chen Xiulong.* Dynamics model of 5-DOF parallel robot mechanism. Transactions of the Chinese Society for Agricultural Machinery, 44(1): 236-243. 2013

[15]. *Chang Boyan, Liu Yanru, Jin Guoguang.* Inverse Dynamics of a 3PUS-S (P) Parallel Metamorphic Mechanism. Transactions of the Chinese Society for Agricultural Machinery, 45(8): 317-323. 2014
[16]. *Tsai L- W.* Solving the Inverse Dynamics of a Stewart- Gough Manipulator by the Principle of Virtual Work. Journal of Mechanical Design, Transactions of the ASME, 122 (1) :3-9. 2000
[17]. *Gallardoj, Ricojm, Frisolia, et al.* Dynamics of Parallel manipulators by means of screw theory. Mechanism and Machine Theory, 38(11):1113-1131. 2003
[18]. *Song Xiaoke, Yang Xiaojun.* Dynamics Analysis of a 4PUS-1RPU Parallel Manipulator by the Principle of Virtual Work. Modular Machine Tool & Automatic Manufacturing Technique, 46 (06):25 - 30. 2012
[19]. *Lee K M, Shah D K.* Dynamic analysis of a three degrees-of-freedom in-parallel actuated manipulator. IEEE Journal of Robotics and Automation, 4(3) : 361-367. 1988
[20]. *Thanh T D, Kotlarski J, Heimann B, et al.* Dynamics identification of kinematically redundant parallel robots using the direct search method. Mechanism and Machine Theory, 55(9): 277-295. 2012
[21]. *Bingyan Cui, Liwen Chen, Zhijun Wang.* Analysis of Statics and Design of Structure Parameters a Bionic Robot Hip Joint. Journal of Biomimetics Biomaterials and Biomedical Engineering, 22:3-12. 2015
[22]. *Cui B Y, Chen L W, Wang Z J, et al.* Design and Dynamic Analysis of a Novel Biomimetic Robotics Hip Joint. Applied Bionics and Biomechanics, 2015(3):1-11. 2015
[23]. *Chen Xu, Deng Liang, Cai Guangqi, Yang Binjiu*. Kinematic analysis for a parallel machine tool based on 3-UPS parallel mechanism. Machinery and electronics, 2005(6):9-11.2005
[24]. *Bingyan Cui, Liwen Chen.* Analysis of kinematic and design of structure parameter for a bionic parallel leg. Journal of Biomimetics, Biomaterials and Biomedical Engineering, 2015(20):23-33. 2015
[25]. *Liwen Chen, Bingyan Cui, Zhijun Wang, et al*. Statics analysis and design of the 6-DOF lower limb bionic leg. Journal of Biomimetics, Biomaterials and Biomedical Engineering, 2016(26):1-12. 2015
[26]. *Rong Yu, Liu Shuangyong, et al*. Dynamics modeling and drive parameter predicion of a 5-DOF wheel grinding manipulator arm. China Mechanical Engineering, 2018, 29(4):449-456. 2018

Glossary of terms

Symbol	Glossary	Symbol	Glossary
$\boldsymbol{\theta}_i$	input angle	$\boldsymbol{P}$	output position parameters
$\boldsymbol{l}_i$	input distance	$\boldsymbol{v}$	output linear velocity
$\boldsymbol{R}$	rotation matrix	$\boldsymbol{r}$	the centroid vector of rod
$\dot{\boldsymbol{\theta}}$	input angle velocity	m	quality
$\boldsymbol{D}$	Jacobian Matrix	$\boldsymbol{J}$	moment of inertia
$\boldsymbol{q}$	generalized coordinates	$\boldsymbol{G}$	force Jacobian Matrix
$\dot{\boldsymbol{q}}$	generalized velocity	T	kinetic energy
$\boldsymbol{F}$	output force	Q	potential energy
$\boldsymbol{H}$	real symmetric inertia matrix	t	time
$\boldsymbol{C}$	coriolis inertia force	g	gravity acceleration
$\boldsymbol{f}$	driver input torque	$\boldsymbol{u}_i$	vector of the frame rotating pair